Published in final edited form as:
Bioorg Med Chem Lett. 2009 October 1; 19(19): 5636–5639. doi:10.1016/j.bmcl.2009.08.051.

Fully automated synthesis and initial PET evaluation of [^{11}C] PBR28

Min Wang[a], **Karmen K. Yoder**[a], **Mingzhang Gao**[a], **Bruce H. Mock**[a], **Xiao-Ming Xu**[b], **Andrew J. Saykin**[a], **Gary D. Hutchins**[a], and **Qi-Huang Zheng**[a,*]

[a]Department of Radiology, Indiana University School of Medicine, 1345 West 16th Street, Room 202, Indianapolis, IN 46202, USA

[b]Department of Neurosurgery, Indiana University School of Medicine, 1345 West 16th Street, Room 202, Indianapolis, IN 46202, USA

Abstract

Fully automated synthesis and initial PET evaluation of a TSPO radioligand, [^{11}C]PBR28 (*N*-(2-[^{11}C]methoxybenzyl)-*N*-(4-phenoxypyridin-3-yl)acetamide), are reported. These results facilitate the potential preclinical and clinical PET studies of [^{11}C]PBR28 in animals and humans.

Keywords

Translocator protein (TSPO); [^{11}C]PBR28; Radiosynthesis; Positron emission tomography (PET); Traumatic brain injury (TBI); Brain imaging

Translocator protein 18 kDa (TSPO, formerly known as the peripheral benzodiazepine receptor)[1] is a protein found in lung, liver, heart, spleen, kidney, adrenals, brain, glial cells, masts cell and macrophages, and is implicated in numerous nervous system disorders such as epilepsy, cerebral ischemia, nerve injury and neurodegenerative diseases, and immune system diseases such as cancer.[2] Brain TSPO density increases in several neuropathological conditions and after experimental injuries to the central nervous system as well.[3] TSPO is an attractive target for molecular imaging of neuroinflammation like Alzheimer's disease and tumor progression using the biomedical imaging technique positron emission tomography (PET).[4] The prototypical TSPO-selective PET radioligand is [^{11}C]PK11195; however, it is reported to have many limitations such as low brain uptake and low sensitivity.[4] These limitations have motivated investigators to search for new TSPO PET radioligands. Promising candidates progressing to human PET studies include [^{11}C]DAA1106, [^{18}F]FEDAA1106 and [^{11}C] PBR28[6-8] as indicated in Figure 1. [^{11}C]PBR28 (*N*-(2-[^{11}C]methoxybenzyl)-*N*-(4-phenoxypyridin-3-yl)acetamide, IC_{50} 0.658 nM) was originally developed by Innis and Pike et al. at the National Institute of Mental Health (NIMH).[8-11] Wishing to study this compound in our laboratory, we investigated a fully automated synthesis of [^{11}C]PBR28 using [^{11}C] methyl triflate ([^{11}C]CH_3OTf)[12,13] and performed initial PET imaging in an animal model of traumatic brain injury (TBI), which overexpresses TSPO.

*Corresponding author. Tel.: +1 317-278-4671. qzheng@iupui.edu (Qi-Huang Zheng)..

The precursor *N*-(2-hydroxybenzyl)-*N*-(4-phenoxypyridin-3-yl)acetamide (desmethyl-PBR28, **4a**) and reference standard *N*-(2-methoxybenzyl)-*N*-(4-phenoxypyridin-3-yl) acetamide (PBR28, **4b**) were prepared according to the procedures outlined in Scheme 1. The route taken was generally based on the literature methods with slight modifications.[11,14,15] Displacement of 4-chloride by phenol was readily achieved by treatment of 4-chloro-3-nitropyridine with phenol in the presence of K_2CO_3 to give 3-nitro-4-phenoxypyridine (**1**) in 97% yield. Reduction of nitro group of compound **1** was performed efficiently with $SnCl_2$ and concentrated HCl instead of 6 N HCl in MeOH to afford 4-phenoxy-3-pyridinamine (**2**)[16] in 92% yield. Condensation of compound **2** with *o*-salicylaldehyde or *o*-anisaldehyde in MeOH, followed by reduction with $NaBH_4$ afforded 2-((4-phenoxypyridin-3-ylamino)methyl)phenol (**3a**) and *N*-(2-methoxybenzyl)-4-phenoxypyridin-3-amine (**3b**) in 91% and 90% yield, respectively. PBR28 (**4b**) was obtained directly by acetylation of the amine **3b** with acetyl chloride in CH_2Cl_2 in 84% yield. Acetylation of the amine and phenolic hydroxyl groups of compound **3a** with acetyl chloride, subsequent hydrolysis of its acetate with LiOH in MeOH provided desmethyl-PBR28 (**4a**) in 78% yield. As depicted in Scheme 2 PBR28 (**4b**) can be achieved by direct *O*-methylation of desmethyl-PBR28 (**4a**) involving anion formation with NaH, followed by CH_3I in DMF in 36% yield.

Synthesis of the target tracer [^{11}C]PBR28 ([^{11}C]**4b**) is indicated in Scheme 3. The phenolic precursor **4a** was labeled using [^{11}C]CH_3OTf[12,13] through *O*-[^{11}C]methylation[17] under basic conditions (NaH) and isolated by a semi-preparative HPLC method[18] to produce the corresponding pure radiolabeled compound [^{11}C]**4b** in 70-80% radiochemical yield, decay corrected to end of bombardment (EOB), based on [^{11}C]CO_2. In comparison with the results reported in the literature,[11] several significant improvements in the radiosynthesis have been made. [^{11}C]CH_3OTf was used as a radiolabeled precursor, which is a proven methylation reagent with greater reactivity than commonly used [^{11}C]methyl iodide ([^{11}C]CH_3I).[11] NaH was used as a strong base instead of $(^tBu)_4NOH$, and CH_3CN was used as the reaction solvent instead of MeOH. The reaction temperature 80 °C was higher than room temperature, and the reaction time was only 3 min, shorter than 7 min in the literature. We also used a “vial” method instead of the reported “loop” method. Therefore, the radiochemical yields for [^{11}C]PBR28 in our method is much higher than that reported previously (26%).[11] The radiosynthesis was performed in an in-house automated multi-purpose ^{11}C-radiosynthesis module, allowing measurement of specific radioactivity during synthesis.[19,20] The overall synthesis, purification and formulation time was 25-30 min from EOB. The specific radioactivity was in a range of 5-15 Ci/μmol at EOB. Chemical purity and radiochemical purity were determined by analytical HPLC.[21] The chemical purity of the precursor and reference standard was > 96%. The radiochemical purity of the target tracer was > 99% determined by radio-HPLC through γ-ray (PIN diode) flow detector, and the chemical purity of the target tracer was >93% determined by reverse-phase HPLC through UV flow detector.

The characterization data for compounds **1-4** and experimental details for the tracer [^{11}C]**4b** are given.[22]

Initial PET evaluation of [^{11}C]PBR28 was performed in rats. Three female Sprague-Dawley rats were imaged. Two animals received a moderate controlled cortical impact (2 mm deformation) to the left parietal cortex (TBI). The third animal received a sham surgery (SHM; incision, skull preparation with no impact). Animals were scanned seven days after surgery. Animals were anesthetized with isoflurane and placed on a stereotaxic-like head-holder.[23] The PET scan was performed right after an intravenous (IV) tail vein injection of 0.31 ± 0.07 mCi [^{11}C]PBR28 (0.58 ± 0.35 nmol/kg). Dynamic data were acquired for 90 minutes on the IndyPET III scanner, a small animal PET scanner designed and developed in the Department of Radiology at Indiana University School of Medicine.[24-26] The raw data collected from 40-90 min was used to generate the images for analysis. Standardized uptake value (SUV) images

were created by normalizing intensity values at each voxel by body weight and injected dose. Regions of interest (ROIs) indicated by the green arrows, approximating the left and right parietal cortices, were drawn on each SUV image. An ellipse (superior-inferior radius = 3 mm; anterior-posterior radius = 4.5 mm) was placed on the approximate anterior-posterior location of the parietal cortex. The ellipse was placed on sequential sagittal slices so that the final ROI spanned the entire lateral to medial extent of each hemisphere. Across all three animals (2 TBI, 1 SHM), SUV values were 16.9 ± 2.23 % higher in the left ROI relative to the right. [^{11}C] PBR28-PET images in 2 TBI and 1 SHM rats are shown in Figure 2.

In conclusion, an efficient and convenient automated synthesis of [^{11}C]PBR28 was developed, and PET evaluation of [^{11}C]PBR28 was performed in a rat model of TBI. These results warrant that the automated preparation of [^{11}C]PBR28 is suitable for preclinical and clinical studies in animals and humans using PET.

Acknowledgments

This work was supported in part by the Indiana Genomics Initiative (INGEN) of Indiana University, as well as by grants from the NIH 5R01AG019771, 3P30AG010133-18S1, 5P50NS052606, and Indiana Economic Development Corporation (IEDC 87884). We gratefully acknowledge Dr. Robert B. Innis at the NIMH for his assistance. The referees' criticisms and editor's comments for the revision of the manuscript are greatly appreciated.

References and notes

1. Papadopoulos V, Baraldi M, Guilarte TR, Knudsen TB, Lacapere J-J, Lindemann P, Norenberg MD, Nutt D, Weizman A, Zhang M-R, Gavish M. Trends Pharmacol.Sci 2006;27:402. [PubMed: 16822554]
2. Wang M, Gao M, Hutchins GD, Zheng Q-H. Eur. J. Med. Chem 2009;44:2748. [PubMed: 18790550]
3. Benavides J, Fage D, Carter C, Scatton B. Brain Res 1987;421:167. [PubMed: 2891401]
4. Probst KC, Izquierdo D, Bird JLE, Brichard L, Franck D, Davis JR, Fryer TD, Richards HK, Clark JC, Davenport AP, Weissberg PL, Warburton EA. Nucl. Med. Biol 2007;34:439. [PubMed: 17499734]
5. Venneti S, Lopresti BJ, Wiley CA. Progr. Neurobiol 2006;80:308.
6. Yasuno F, Ota M, Kosaka J, Ito H, Higuchi M, Doronbekov TK, Nozaki S, Fujimura Y, Koeda M, Asada T, Suhara T. Biol. Psychiatry 2008;64:835. [PubMed: 18514164]
7. Fujimura Y, Ikoma Y, Yasuno F, Suhara T, Ota M, Matsumoto R, Nozaki S, Takano A, Kosaka J, Zhang MR, Nakao R, Suzuki K, Kato N, Ito H. J. Nucl. Med 2006;47:43. [PubMed: 16391186]
8. Brown AK, Fujita M, Fujimura Y, Liow JS, Stabin M, Ryu YH, Imaizumi M, Hong J, Pike VW, Innis RB. J. Nucl. Med 2007;48:2072. [PubMed: 18006619]
9. Imaizumi M, Kim HJ, Zoghbi SS, Briard E, Hong J, Musachio JL, Ruetzler C, Chuang DM, Pike VW, Innis RB, Fujita M. Neurosci. Lett 2007;411:200. [PubMed: 17127001]
10. Imaizumi M, Briard E, Zoghbi SS, Gourley JP, Hong J, Fujimura Y, Pike VW, Innis RB, Fujita M. Neuroimage 2008;39:1289. [PubMed: 18024084]
11. Briard E, Zoghbi SS, Imaizumi M, Gourley JP, Shetty HU, Hong J, Cropley V, Fujita M, Innis RB, Pike VW. J. Med. Chem 2008;51:17. [PubMed: 18067245]
12. Jewett DM. Int. J. Radiat. Appl. Instrum. A 1992;43:1383.
13. Mock BH, Mulholland GK, Vavrek MJ. Nucl. Med. Biol 199926:467.
14. Wilson AA, Garcia A, Parkes J, McCormick P, Stephenson KA, Houle S, Vasdev N. Nucl. Med. Biol 2008;35:305. [PubMed: 18355686]
15. Okubo T, Yoshikawa R, Chaki S, Okuyama S, Nakazato A. Bioorg. Med. Chem 2004;12:3569. [PubMed: 15186841]
16. Elslager EF, Clarke J, Werbel LM, Worth DF. J. Med. Chem 1972;15:827. [PubMed: 4625530]
17. Zheng Q-H, Liu X, Fei X, Wang J-Q, Ohannesian DW, Erickson LC, Stone KL, Hutchins GD. Nucl. Med. Biol 2003;30:405. [PubMed: 12767398]

18. Wang M, Lacy G, Gao M, Miller KD, Sledge GW, Zheng Q-H. Bioorg. Med. Chem. Lett 2007;17:332. [PubMed: 17095221]
19. Mock BH, Zheng Q-H, DeGrado TR. J. Label. Compd. Radiopharm 2005;48:S225.
20. Mock BH, Glick-Wilson BE, Zheng Q-H, DeGrado TR. J. Label. Compd. Radiopharm 2005;48:S224.
21. Zheng Q-H, Mock BH. Biomed. Chromatogr 2005;19:671. [PubMed: 15803445]
22. (a). Compound **1**, a pale yellow solid, mp 70-71 °C (lit.[10] 75 °C). ^{1}H NMR ($CDCl_3$, 500 MHz): δ 9.14 (s, 1H), 8.55 (d, *J* = 6.0 Hz, 1H), 7.52-7.48 (m, 2H), 7.37-7.34 (m, 1H), 7.17-7.15 (m, 2H), 6.79 (d, *J* = 6.0 Hz, 1H). Compound **2**, a red oil. ^{1}H NMR ($CDCl_3$, 500 MHz): δ 8.17 (s, 1H), 7.89 (d, *J* = 5.5 Hz, 1H), 7.43-7.39 (m, 2H), 7.24-7.21 (m, 1H), 7.10-7.07 (m, 2H), 6.58 (d, *J* = 5.5 Hz, 1H), 3.95 (br s, 2H). Compound **3a**, a white solid, mp 193-194 °C (lit.[10] 180-182 °C). ^{1}H NMR (DMSO-d_6, 500 MHz): δ 9.62 (br s, 1H), 7.86 (s, 1H), 7.70 (d, *J* = 5.5 Hz, 1H), 7.47-7.44 (m, 2H), 7.23 (t, *J* = 7.5 Hz, 1H), 7.19 (d, *J* = 7.0 Hz, 1H), 7.12 (d, *J* = 8.0 Hz, 2H), 7.07-7.04 (m, 1H), 6.83 (d, *J* = 7.5 Hz, 1H), 6.74 (t, *J* = 7.5 Hz, 1H), 6.54 (d, *J* = 5.5 Hz, 1H), 5.93 (t, J = 6.5 Hz, 1H), 4.35 (d, J = 6.5 Hz, 2H). LC/MS (*m/z*, ESI): $[M+H]^+$ calcd for $C_{18}H_{17}N_2O_2$ 293.1, found 293.0. Compound **3b**, a pale yellow oil. ^{1}H NMR ($CDCl_3$, 500 MHz): δ 8.09 (s, 1H), 7.84 (d, *J* = 5.5 Hz, 1H), 7.41-7.37 (m, 2H), 7.32-7.31 (m, 1H), 7.28-7.24 (m, 1H), 7.22-7.19 (m, 1H), 7.07-7.04 (m, 2H), 6.94-6.88 (m, 2H), 6.54 (d, *J* = 5.5 Hz, 1H), 4.73 (t, *J* = 5.5 Hz, 1H), 4.45 (d, *J* = 6.0 Hz, 2H), 3.83 (s, 3H). LC/MS (*m/z*, ESI): $[M+H]^+$ calcd for $C_{19}H_{19}N_2O_2$ 307.1, found 307.1. Compound **4a**, a white solid, mp 123-124 °C (lit.[10] 123-125 °C). ^{1}H NMR ($CDCl_3$, 500 MHz): δ 9.07 (br s, 1H), 8.48 (d, *J* = 5.5 Hz, 1H), 8.43 (s, 1H), 7.41 (t, *J* = 8.0 Hz, 2H), 7.30 (t, *J* = 7.5 Hz, 1H), 7.23-7.20 (m, 1H), 6.94 (d, *J* = 8.0 Hz, 1H), 6.79-6.72 (m, 5H), 4.94 (d, *J* = 14.5 Hz, 1H), 4.79 (d, *J* = 15.0 Hz, 1H), 2.05 (s, 3H). LC/MS (*m/z*, ESI): $[M+H]^+$ calcd for $C_{20}H_{19}N_2O_3$ 335.1, found 335.1. Compound **4b**, a white solid, mp 84-85 °C (lit.[9] 89-91 °C). ^{1}H NMR ($CDCl_3$, 500 MHz): δ 8.28 (d, *J* = 5.5 Hz, 1H), 8.21 (s, 1H), 7.44-7.40 (m, 2H), 7.39-7.37 (m, 1H), 7.29-7.28 (m, 1H), 7.24-7.20 (m, 1H), 6.95-8.86 (m, 3H), 6.74 (d, *J* = 8.0 Hz, 1H), 6.57 (d, *J* = 5.5 Hz, 1H), 5.14 (d, *J* = 14.5 Hz, 1H), 4.89 (d, *J* = 14 Hz, 1H), 3.58 (s, 3H), 1.99 (s, 3H). LC/MS (*m/z*, ESI): $[M+H]^+$ calcd for $C_{21}H_{21}N_2O_3$ 349.1, found 349.0. (b). Production of the tracer [^{11}C]PBR28 ([^{11}C]**4b**). [^{11}C]CO_2 was produced by the ^{14}N(p,α)^{11}C nuclear reaction in small volume (9.5 cm^3) aluminum gas target (CTI) from 11 MeV proton cyclotron on research purity nitrogen (+1% O_2) in a Siemens radionuclide delivery system (Eclipse RDS-111). In a small reaction vial (5 mL), the precursor **4a** (0.5-1.0 mg) was dissolved in CH_3CN (300 μL). To this solution was added NaH (1 mg). No carrier-added (high specific activity) [^{11}C]CH_3OTf that was produced by the gas-phase production method[13] from [^{11}C]CO_2 through [^{11}C]CH and [^{11}C]CH_3Br with silver triflate (AgOTf) column was passed into the reaction vial at rt, until radioactivity reached a maximum (~2 min), and then the reaction vial was isolated and reacted at 80 °C for 3 min. The contents of the reaction vial were diluted with $NaHCO_3$ (1 mL, 0.1 M), and injected onto the semi-preparative HPLC column with 2 mL injection loop for purification, which we used a Prodigy (Phenomenex), S-5 μm, 12 nm, 10 × 250 mm i.d. C-18 column; 52% CH_3CN/H_2O mobile phase; flow rate 5.0 mL/min; and UV (254 nm) and γ-ray (PIN diode) flow detectors. The product fraction was collected, the solvent was removed by rotatory evaporation under vacuum, and the final product, [^{11}C]PBR28 ([^{11}C]**4b**), was formulated in saline, sterile-filtered through a sterile vented Millex-GS 0.22 μm cellulose acetate membrane, and collected into a sterile vial. Total radioactivity was assayed and total volume was noted for dose dispensing. The overall synthesis, purification and formulation time was 25-30 min from EOB. Retention times in the analytical HPLC, which we used a Prodigy (Phenomenex) 5 μm C-18 column, 4.6 × 250 mm; 52% CH_3CN/H_2O mobile phase; flow rate 1.0 mL/min; and UV (254 nm) and γ-ray (PIN diode) flow detectors, were: t_R **4a** = 6.51 min, t_R **4b** = 7.57 min, t_R [^{11}C]**4b** = 7.57 min. Retention times in the semi-preparative HPLC were: t_R **4a** = 6.50 min, t_R **4b** = 7.98 min, t_R [^{11}C]**4b** = 7.98 min. The radiochemical yields were 70-80% decay corrected to EOB, based on [^{11}C]CO_2.
23. Cheng TE, Yoder KK, Normandin MD, Risacher SL, Converse AK, Hampel JA, Miller MA, Morris ED. J. Neurosci. Methods 2009;176:24. [PubMed: 18824025]
24. Frese T, Rouze NC, Bouman CA, Sauer K, Hutchins GD. IEEE Trans. Med. Imaging 2003;22:258. [PubMed: 12716002]
25. Rouze NC, Hutchins GD. IEEE Trans. Nucl. Sci 2003;50:1491.
26. Rouze NC, Soon VC, Young JW, Siegel S, Hutchins GD. IEEE Nucl. Sci. Symposium Conference Record 2005;4:2394.

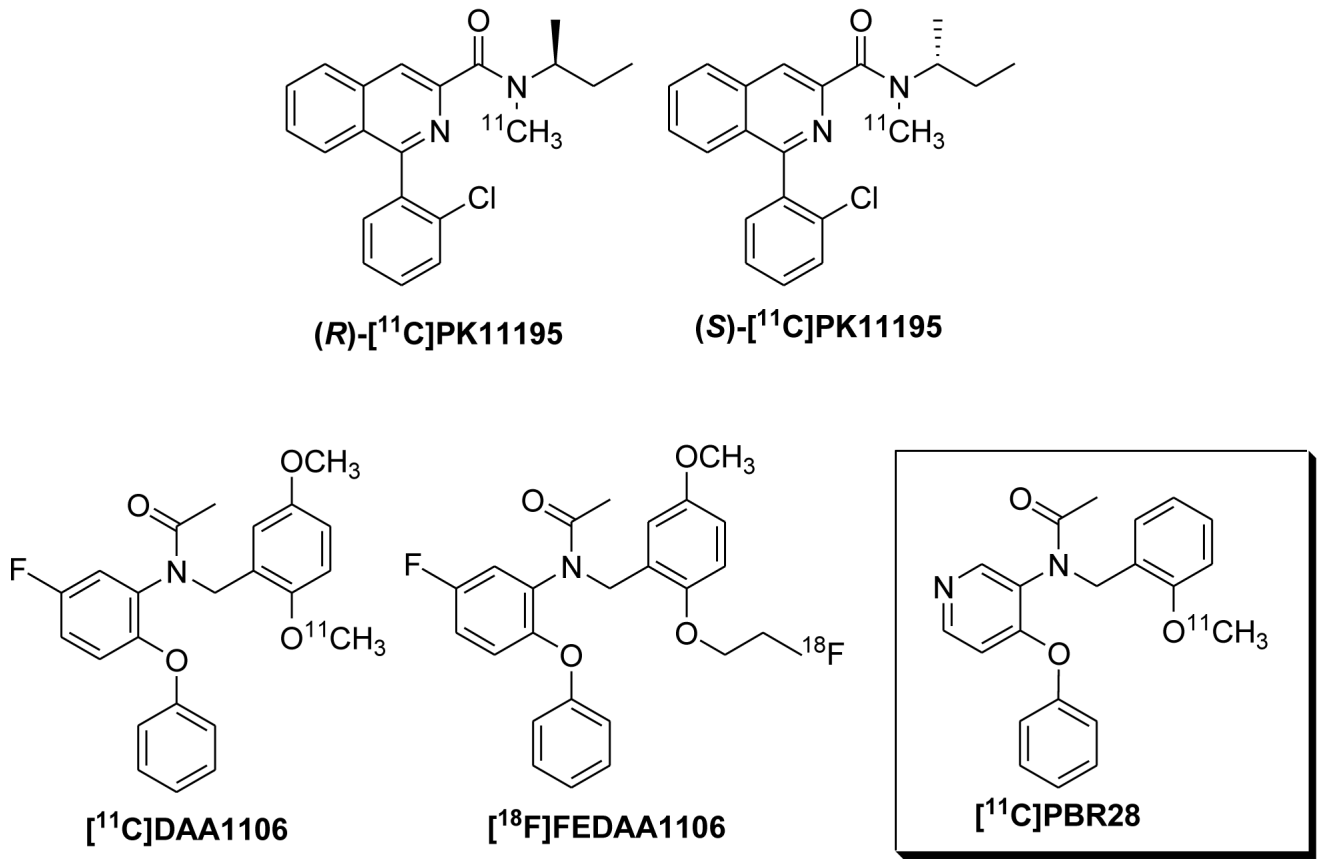

Figure 1.
Chemical structures of PET TSPO radioligands.

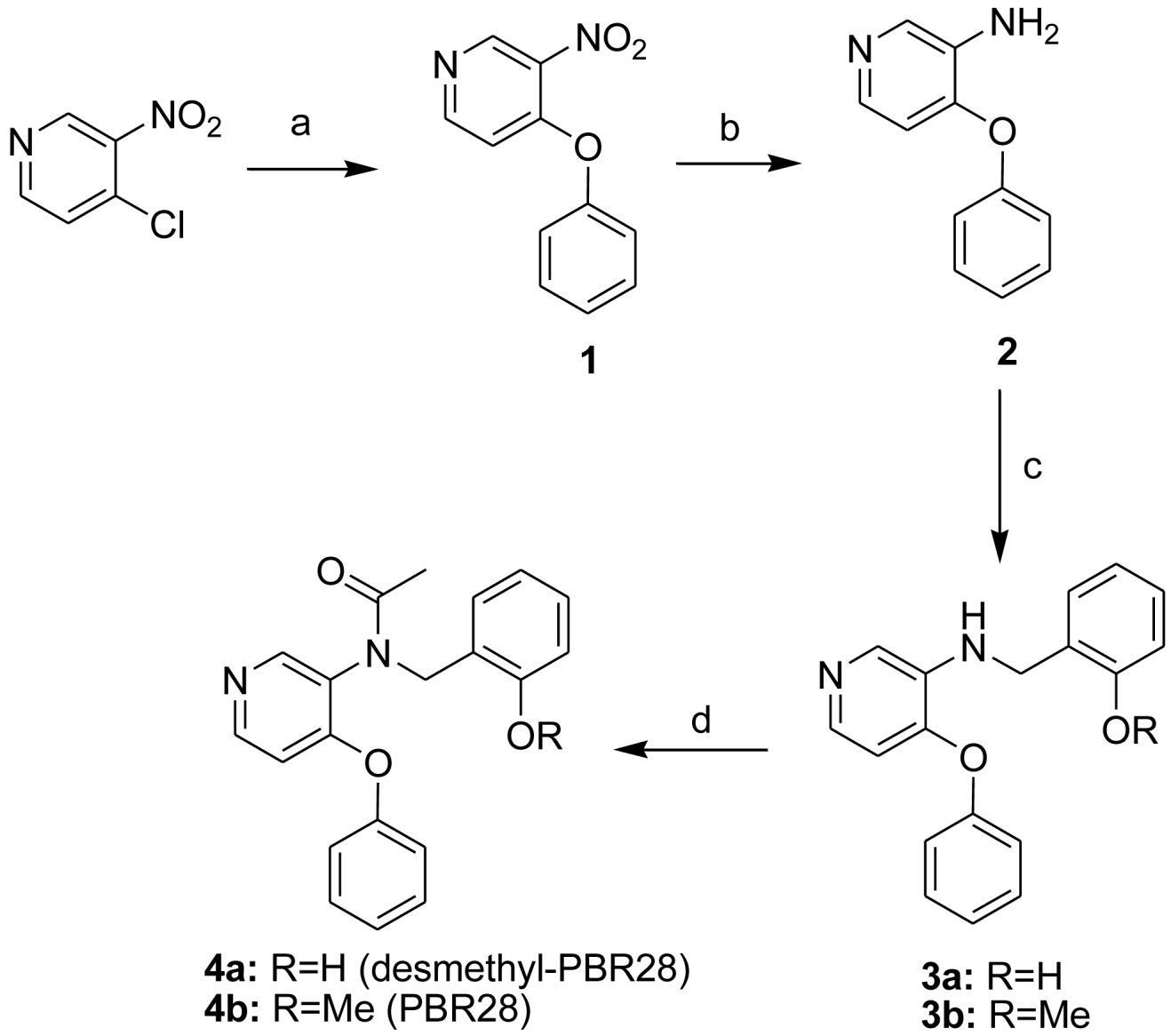

Scheme 1.

Synthesis of desmethyl-PBR28 and PBR28. Reagents, conditions, and yields: (a) phenol, K_2CO_3, DMF, 80°C, 97%; (b) $SnCl_2$, conc. HCl, MeOH, 80°C, 92%; (c) for **3a**: *o*-salicylaldehyde, 90°C, then $NaBH_4$, MeOH, room temperature (rt), 91%; for **3b**: *o*-anisaldehyde, 100°C; then $NaBH_4$, MeOH, rt, 90%; (d) for **4a**: acetyl chloride, DMAP, CH_2Cl_2, rt, then sat. LiOH, MeOH, rt, 84%; for **4b**: acetyl chloride, DMAP, CH_2Cl_2, rt, 78%.

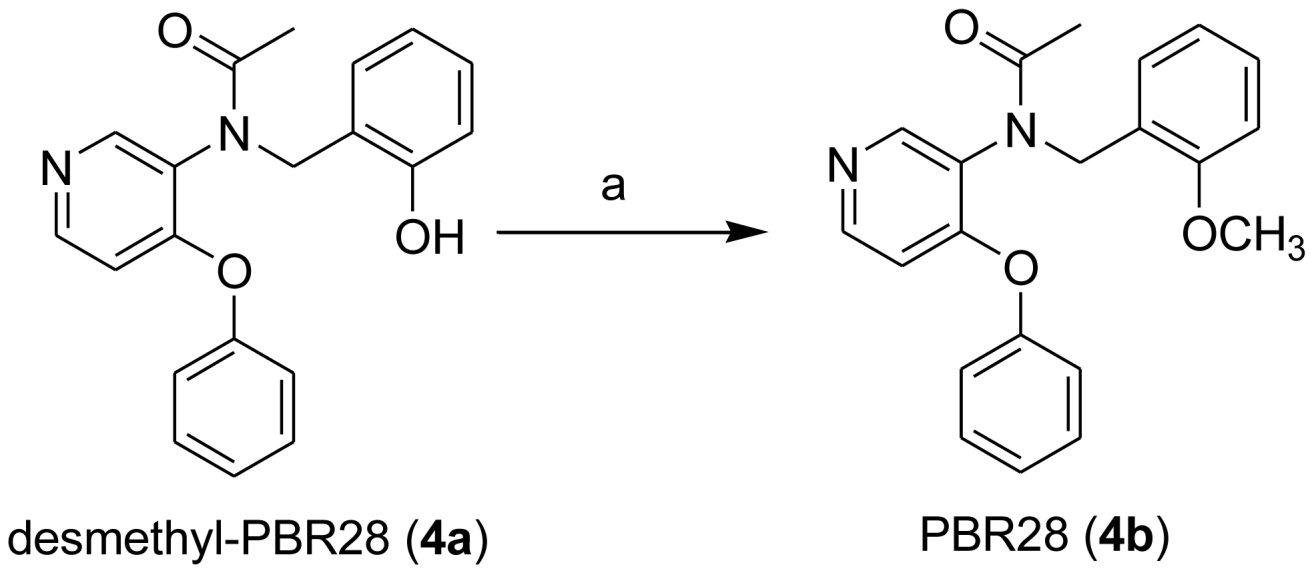

desmethyl-PBR28 (**4a**) PBR28 (**4b**)

Scheme 2.

Alternate synthetic approach for PBR28. Reagents, conditions, and yields: (a) NaH, CH_3I, DMF, rt, 36%.

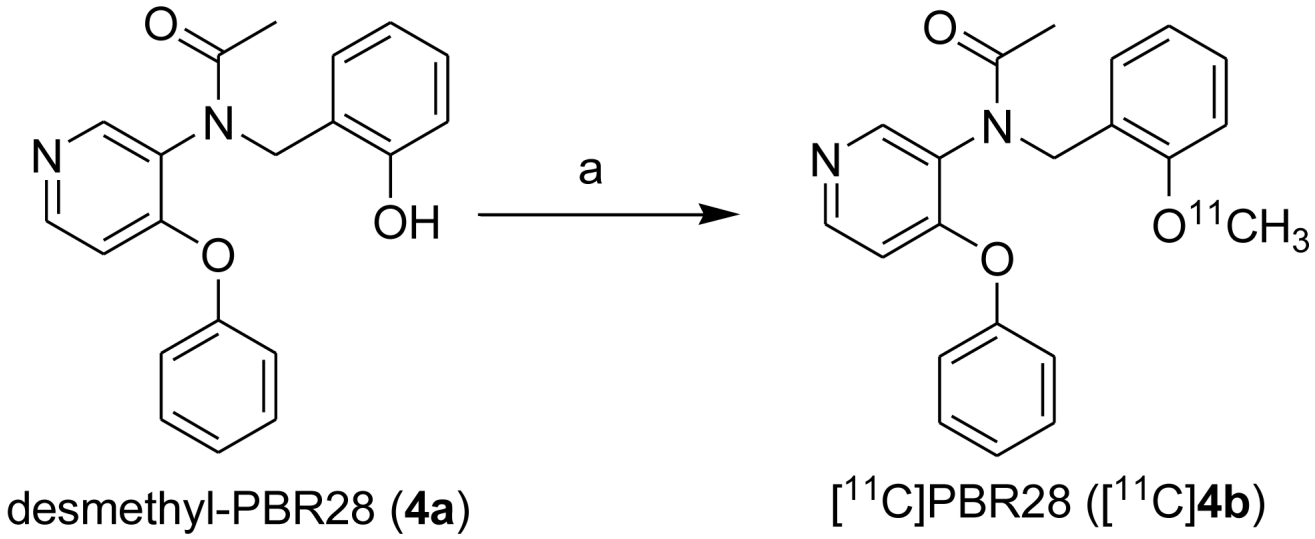

Scheme 3.
Synthesis of [^{11}C]PBR28. Reagents, conditions, and yields: (a) NaH, [^{11}C]CH_3OTf, CH_3CN, 80 °C, 3 min, 70-80%.

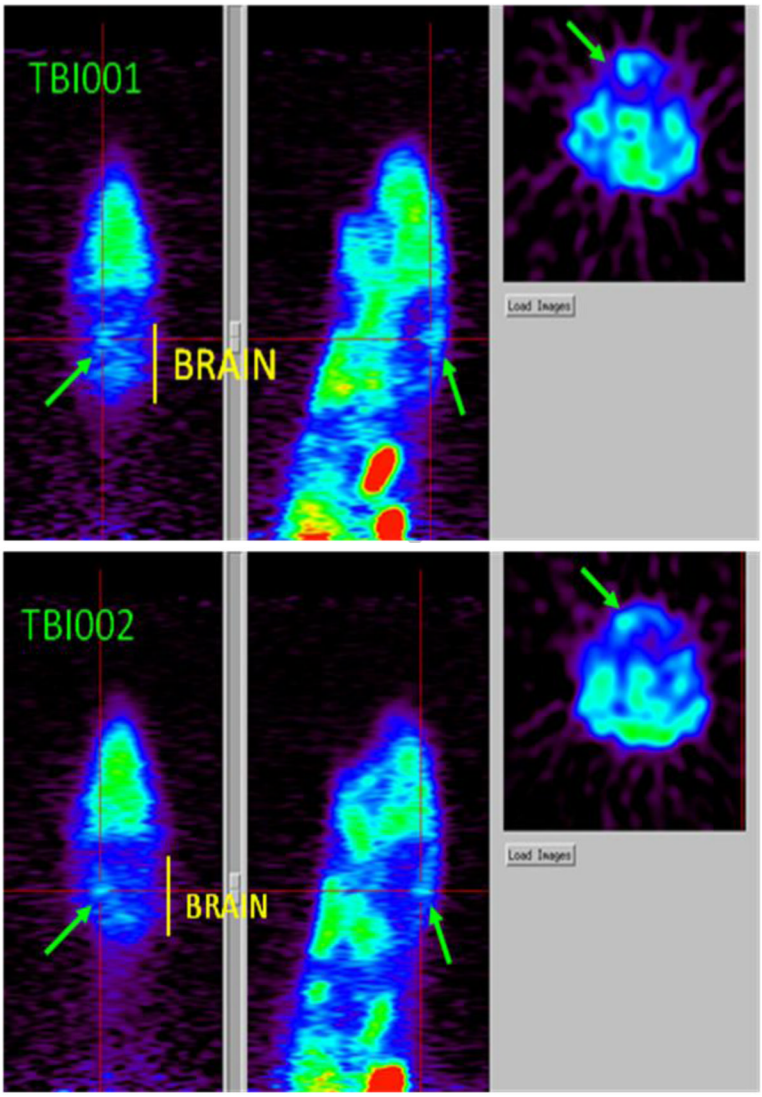

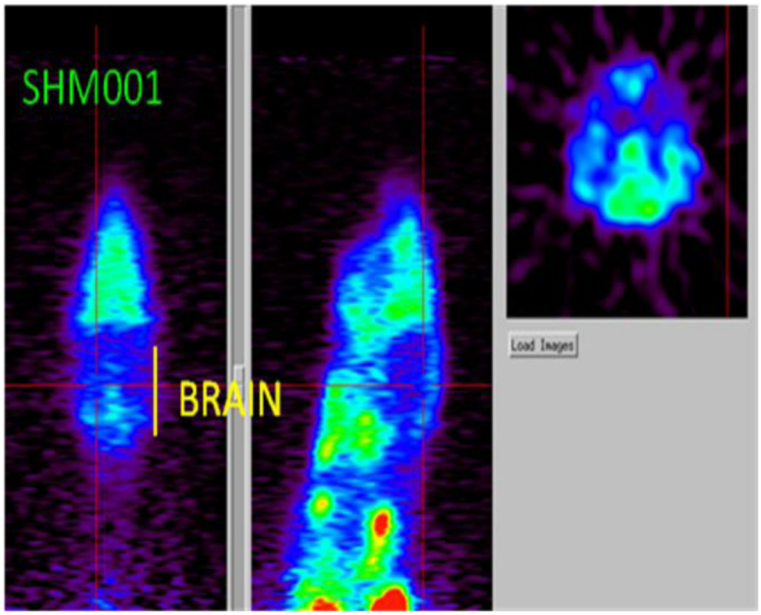

Figure 2.
[^{11}C]PBR28-PET images in 2 TBI and 1 SHM rats.
A. TBI.001. 40-90 min integrated image. Crosshairs positioned at putative site of lesion: left parietal cortex. Green arrows indicated ROIs in the rat brain.
B. TBI.002. 40-90 min integrated image. Crosshairs positioned at putative site of lesion: left parietal cortex. Green arrows indicated ROIs in the rat brain.
C. SHM.001. 40-90 min integrated image. Crosshairs positioned at roughly the same coordinates as in **A** and **B**. In this animal, there was no visible left-side lesion.